Identification of the Brillouin zone planes in the Hume-Rothery matching rule and their role in the formation of the pseudogap from *ab initio* band calculations for the Al-Mg-Zn 1/1-1/1-1/1 approximant

Hirokazu Sato,[1] Tsunehiro Takeuchi,[2] and Uichiro Mizutani[2]
[1]*Department of Physics, Aichi University of Education, Kariya 448-8542, Japan*
[2]*Department of Crystalline Materials Science, Nagoya University, Nagoya 464-8603, Japan*
(Received 4 December 2000; revised manuscript received 9 May 2001; published 15 August 2001)

The Hume-Rothery matching rule has been widely used for many years as a practically useful guide to search for new quasicrystals and their approximants. In this work, we have performed the linear muffin-tin orbital atomic-sphere approximation band calculations for the nearly-free-electron-like $Al_{30}Mg_{40}Zn_{30}$ 1/1-1/1-1/1 approximant. It is shown that highly degenerate free-electron states in the vicinity of the center of (543), (710), and (550) planes, whose reciprocal lattice vectors well coincide with the Fermi diameter $2k_F$ in the extended zone scheme, are all reduced to the regions centered at the point *N* corresponding to the center of the (110) zone planes in the reduced-zone scheme and that the lifting of these degenerate states leads to the sizable pseudogap at the Fermi level, thereby lowering the electronic energy in this system. This is, to our knowledge the first attempt to identify the Brillouin zone planes in the empirical Hume-Rothery rule and to extract their role in the formation of the pseudogap from *ab initio* band calculations.

DOI: 10.1103/PhysRevB.64.094207 PACS number(s): 61.44.Br

I. INTRODUCTION

Icosahedral quasicrystals (QC's) are divided into two families in terms of the cluster unit building up their structure: one is described by the Mackay icosahedron containing 54 atoms and the other is described by the rhombic triacontahedron containing 45 atoms. The former abbreviated as MI-type QC's contains the transition-metal (TM) elements as major components. Tsai *et al.*[1] discovered a series of thermally stable Al-Cu-TM (TM=Fe, Ru, Os) MI-type QC's and pointed out that they are formed at a specific electron per atom ratio e/a of about 1.75. Guided by this empirical rule, Yokoyama *et al.*[2] could further synthesize thermally stable Al-Pd-TM QC's at an e/a ratio of around 1.75. Their successive discoveries convinced us to believe that the thermally stable QC's obey well the Hume-Rothery rule and that the QC is apparently stabilized by matching the Fermi surface with the Brillouin-zone planes specific to the respective QC's and lowering the electronic energy as a consequence of the formation of the pseudogap at the Fermi level.

The rhombic-triacontahedral-type QC's (hereafter abbreviated as RT type) belong to the second family together with their 1/1-1/1-1/1 cubic approximants (RT type AC's). They have been also known as being typical of Hume-Rothery-type electron compounds. For example, the measured electronic specific-heat coefficient, when plotted against e/a, is found to fall on a universal curve and to decrease with decreasing e/a value toward 2.1 regardless of the atomic species involved.[3] Typical examples in this family include Al-Mg-Zn, Al-Li-Cu, and Al-Mg-*X* (*X*=Cu, Ag, and Pd). The electron concentration or the electron per atom ratio e/a in RT-type QC's and AC's, except for those containing Pd, can be unambiguously assigned and the nearly-free-electron-like valence-band structure is expected because of the absence of the transition-metal elements.

Takeuchi and Mizutani[4] studied more systematically the electronic structure and electron transport properties for a series of the nearly-free-electron-like Al-Mg-Zn QC's and AC's and revealed the pseudogap at the Fermi level for all QC's and AC's they studied by measuring the x-ray photoemission spectroscopic valence-band structure and the electronic specific-heat coefficient. Here it is interesting to note that its depth is deeper in QC's than in AC's. They also noted that, in the respective stable concentration ranges, the diameter of the free-electron Fermi sphere $2k_F$ matches well the reciprocal lattice vectors K_{543}, K_{710}, and K_{550} corresponding to the strong x-ray diffraction peaks in the AC's and K_{222100} in the case of the QC's. They conjectured that the pseudogap at the Fermi level is brought about by the Fermi-surface-Brillouin-zone interaction caused by the Hume-Rothery matching rule mentioned above. Unfortunately, however, their discussion was limited to a qualitative evaluation based on the $2k_F=K_{hkl}$ matching rule, where (hkl) refer to the Miller indices of the set of lattice planes.

The electronic structure of QC's has been alternatively studied from the first-principle band calculations. Because of the possession of an infinitely large unit cell in QC's, the band calculations have been performed only for AC's whose atomic structure was constructed by a model structure. Fujiwara[5] calculated the valence band by constructing a model structure on the basis of the α-phase Al-Mn-Si compound, which is known as the 1/1-1/1-1/1 approximant to the Al-Mn quasicrystal. The calculated density of states (DOS) turned out to consist of a series of spiky peaks with the possession of the pseudogap at the Fermi level. He suggested the location of the Fermi level in the pseudogap to contribute to lowering the electronic energy in favor of a quasicrystal. Since then, theoretical band calculations have been performed for a number of approximants including RT-type AC's like Al-Li-Cu (Ref. 6) and Al-Mg-Zn.[7] All results so far reported are consistent with the finding of the pseudogap at the Fermi level. In particular, Hafner and Krajčí[7] obtained

essentially the same results for higher-order approximants and claimed that the pseudogap is a feature commonly existing in quasicrytals and their approximants.

The successful application of the Hume-Rothery matching rule to the search for new stable quasicrystals by Tsai and others has certainly stimulated theoretical interest in the mechanism of the Hume-Rothery rule. The role of the diffraction by Bragg planes in the Al-Li-Cu icosahedral quasicrystal has been studied by Friedel and Denoyer.[8] Smith and Ashcroft[9] applied the pseudopotential method to a simplified three-dimensional Penrose tiling structure and revealed the appearance of band gaps associated with quasicrystal reciprocal-lattice vectors and van Hove singularities in the density of states. Vaks *et al.*[10] elaborated the work by Smith and Ashcroft above and studied the Hume-Rothery-type correlations, i.e., a connection between the valency calculated from a Fermi sphere with a radius having one-half the reciprocal-lattice vector and the nominal mean valency. Trambly de Laissardiére *et al.*[11] performed the self-consistent linear muffin-tin orbital (LMTO) band calculations for a series of Hume-Rothery crystals containing a small concentration of transition-metal elements to extract the role of the transition-metal element in the depth of the pseudogap near the Fermi level. More recently, Fournée *et al.*[12] made the augmented-plane-wave band calculations for Al-Cu alloys and discussed the Hume-Rothery criterion in comparison with the experimental data obtained from soft x-ray spectroscopies. However, a straightforward identification of Brillouin-zone planes responsible for the formation of the pseudogap at E_F has not been pursued in the past from *ab initio* band calculations.

In the present work, the band calculations have been carried out for the $Al_{30}Mg_{40}Zn_{30}$ 1/1-1/1-1/1 approximant whose atomic structure had been accurately determined from the Rietveld analysis.[13] The origin of the pseudogap found across the Fermi level is discussed by analyzing the calculated energy-dispersion curves, DOS, and the Fermi surfaces in comparison with those derived from the free-electron model in both reduced- and extended-zone schemes. We demonstrate the pseudogap across the Fermi level in the Al-Mg-Zn approximant to originate from the interaction of the Fermi surface with the Brillouin zone formed by (543), (710), and (550) planes, which are already known to satisfy the Hume-Rothery matching rule.[4]

II. ATOMIC STRUCTURE OF THE $Al_{30}Mg_{40}Zn_{30}$ 1/1-1/1-1/1 APPROXIMANT

According to the powdered x-ray diffraction Rietveld analysis,[13] the $Al_{30}Mg_{40}Zn_{30}$ AC is found to belong to the space group $Im\bar{3}$ and to crystallize into the bcc structure with the lattice constant 14.355 Å. The atomic structure thus determined is listed in Table I. It contains totally 160 atoms in its unit cell and the center of the icosahedral clusters at both vertex and center sites is essentially vacant. It is also found that a chemical disordering exists in the first icosahedral shell and outer shells, where Al and Zn atoms are occupied. There is no chemical disorder in the Mg site.

TABLE I. Atomic structure for the $Al_{30}Mg_{40}Zn_{40}$ 1/1-1/1-1/1 approximant (Ref. 13) Space group; $Im\bar{3}$; lattice constant $a = 14.355$ Å; number of atoms per unit cell $N = 160$; x, y, z, coordinates of atom positions normalized with respect to a; s, atomic radius normalized with respect to a.

Atoms	Site	x	y	z	s
Al	2*a*	0.0000	0.0000	0.0000	0.0975
Mg	48*h*	0.1579	0.1904	0.4030	0.1122
Mg	12*e*	0.4030	0.0000	0.5000	0.1181
Mg	12*e*	0.1978	0.0000	0.5000	0.1174
Mg	16*f*	0.0000	0.3009	0.1175	0.1193
Zn	24*g*	0.0000	0.0927	0.1514	0.1073
Zn	24*g*	0.0000	0.1775	0.3061	0.1117

III. CONSTRUCTION OF THE FERMI SPHERE AND BRILLOUIN ZONE IN THE EXTENDED SCHEME

As noted in the Introduction, experimentalists generally test the Hume-Rothery matching rule $2k_F = K_{hkl}$ in the discussion of the phase stability and evaluate the ratio of the Fermi diameter $2k_F$ over the reciprocal-lattice vector K_{hkl} corresponding to strong x-ray diffraction lines.[1,2,4] Indeed, we can easily confirm that the (543), (550), and (710) zone planes are located close to the Fermi sphere with its radius k_F of 1.554 $Å^{-1}$ calculated from the free-electron model for the $Al_{30}Mg_{40}Zn_{30}$ AC with the e/a value of 2.3.[4] To illustrate this visually, we depict in Fig. 1 the three-dimensional Brillouin zone formed by 48-fold (543), 12-fold (550), and 24-fold (710) planes, all of which are located at the same distance from the origin, i.e., $\pi\sqrt{h^2+k^2+l^2}/a = \pi\sqrt{50}/14.355 \cong 1.548$. The Brillouin zone and spherical Fermi sphere in the extended-zone scheme were constructed by using the software developed by Nakano *et al.*[14] As illustrated in Fig. 1, the overlap of the free-electron Fermi sphere across the zone centers simultaneously occurs at 84 zone planes, since the energy gap across the zones is absent in the free-electron model. Thus, we consider such high multiplicity of zone

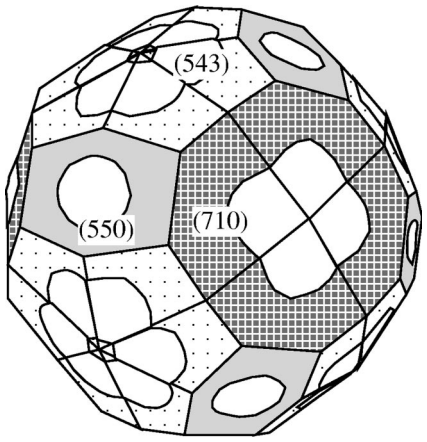

FIG. 1. The Brillouin zone consisting of (543), (550), and (710) planes with the free-electron Fermi sphere in the Al-Mg-Zn 1/1-1/1-1/1 approximant. The overlap of the Fermi sphere is slightly exaggerated by taking $k_F = 1.569$ $Å^{-1}$ and $K_{hkl}/2 = 1.548$ $Å^{-1}$.

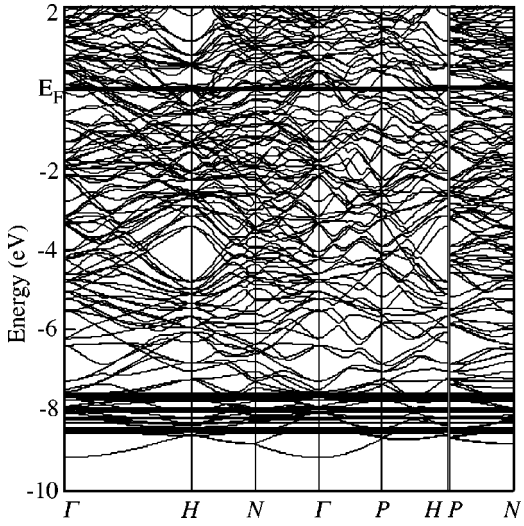

FIG. 2. Dispersion relations in the reduced-zone scheme for the $Al_{30}Mg_{40}Zn_{30}$ 1/1-1/1-1/1 approximant.

planes to produce a sizable pseudogap near the Fermi level. As our next objective, we examine how the Fermi-surface-Brillouin-zone interaction in the extended-zone scheme discussed above can be reconciled with *ab initio* band calculations.

IV. BAND CALCULATIONS FOR THE $Al_{30}Mg_{40}Zn_{30}$ 1/1-1/1-1/1 APPROXIMANT

The band calculations have been performed for the present approximant within the context of the LMTO atomic-sphere Approximation (ASA) in combination with the local density-functional theory.[15,16] As noted above, there exists chemical disorder in the occupation of Al and Zn atoms. Since the band calculations generally do not allow chemical disordering in the unit cell, we filled only Zn atoms in the first icosahedral shell and rhombic triacontahedral shell while only Al atoms in the remaining outer shells. This can be done without changing the overall composition. Though the chemical disorder was removed, we still employed atom positions listed in Table I, which were experimentally determined for the chemically disordered real $Al_{30}Mg_{40}Zn_{30}$ AC. The atomic radius s for the constituent atom, which is listed in the last column in Table I, was assumed to be given by that of an atomic sphere having the same volume as the corresponding Voronoi polyhedron. The potential parameters were determined self-consistently at 91 independent $\boldsymbol{k}$ points in the irreducible wedge of the Brillouin zone of the bcc structure. The DOS turned out to be sufficiently accurate when energy eigenvalues were calculated at these 91 $\boldsymbol{k}$ points in the irreducible part of the zone. In the case of energy dispersions, however, energy eigenvalues along a given direction were calculated at more than 300 $\boldsymbol{k}$ points to make the dispersion relation smooth.

The energy dispersion relations for the present AC are presented in Fig. 2 in the reduced-zone scheme. The valence band-structure is formed by a mixture of $3s$, $3p$, $3d$ extended states of Al and Mg atoms and $4s$ and $4p$ states of Zn atoms. The narrow Zn-$3d$ states are formed at the bottom of the valence band. Thus, the valence band structure is essentially described in terms of the nearly-free-electron model. The resulting DOS is shown in Fig. 3. We clearly see the pseudogap in the calculated DOS across the Fermi level. Admittedly, however, the formation of the pseudogap is not so obviously judged from the dispersion relations shown in Fig. 2. Thus, more deliberate consideration was made to identify its origin.

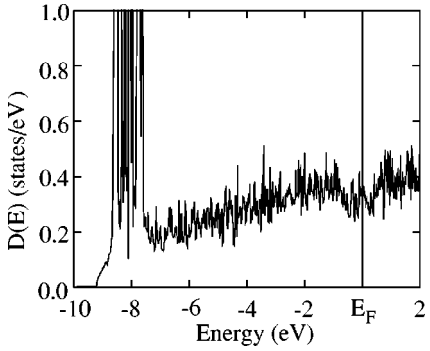

FIG. 3. Density of states calculated in the framework of the LMTO-ASA method for the $Al_{30}Mg_{40}Zn_{30}$ 1/1-1/1-1/1 approximant.

Energy dispersions derived from both LMTO-ASA and the free-electron model along the directions pointing to the center N of the (543), (550), and (710) zone planes were calculated in the extended-zone scheme in order to single out the effect of these zone planes on the electronic states near the Fermi level. We show in Figs. 4(a), 4(b), and 4(c) the superposition of LMTO-ASA and free-electron dispersions along (543), (550), and (710) reciprocal-lattice vectors in the vicinity of the Fermi energy and the point N, respectively. It is seen that a number of free-electron parabolas meet at the point N corresponding to the (543), (550), and (710) zone centers and that the number of the degenerate states increases with increasing energy. Indeed, we see from Fig. 4 that in all three cases, the Fermi level happens to pass very near the most degenerate free-electron states at the point N but that these degenerate states are lifted in the LMTO-ASA band calculations. Therefore, we can safely say that the appearance of the energy gaps across the (543), (550), and (710) zone planes, though they are rather small, must play a key role in the formation of the pseudogap at the Fermi level.

Because of the zone-folding effect, electronic states after lifting the degeneracy are found to be quite flat and densely separated in energy with the width of 0.1 to 0.2 eV. This certainly yields spiky peaks in the calculated DOS. It is therefore not obvious to conclude if the lifting of the highly degenerate free-electron states at the point N immediately leads to a sizable pseudogap across the Fermi level. To clarify this, we intentionally deleted, from the free-electron band, the states in the region centered at the point N where the condition $h^2+k^2+l^2=50$ is satisfied. This will allow us to evaluate quantitatively the depth of the pseudogap caused by the lifting of the highly degenerate states near the point N. Figure 5 shows the free-electron DOS with and without deletion of the electronic states around the point N enclosed by a sphere in radius Δk. This is done by using the free-electron

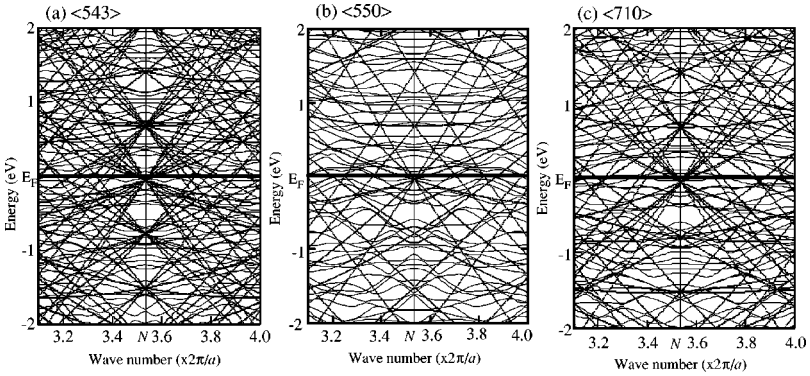

FIG. 4. Dispersion relations derived from LMTO-ASA and free-electron model (dotted line) in the extended zone scheme along (a) ⟨543⟩, (b) ⟨550⟩, and (c) ⟨710⟩ directions. The wave number is in the units of $2\pi/a$ and the point N is positioned at $\sqrt{50}/2=3.53$.

dispersion relations in the extended-zone scheme. It is clear that the depth of the pseudogap across the Fermi level becomes comparable to that shown in Fig. 3 when $\Delta k=0.2$ in the units of $2\pi/a$ is chosen. In addition, as shown in its inset, the respective contributions to DOS at the Fermi level from (543), (710), and (550) planes are 4:2:1, in excellent agreement with their degeneracies of 48:24:12. Though energy gaps across these three sets of planes are certainly not necessarily equal, we believe that the total lifting of 84-fold degeneracy at the point N is strong enough to cause the pseudogap across the Fermi level.

To ascertain the origin of the pseudogap further, we calculated the cross section of the Fermi surfaces in the k_xk_y plane in the reduced-zone scheme. Prior to the discussion of the resulting Fermi surfaces, we should note that the zone planes in the extended-zone scheme, when reduced to the first zone, always pass the point N corresponding to the center of the (110) zone, when two of the Miller indices of the reciprocal lattice vector (hkl) are odd like (543), (550), and (710) in the present case. It is also easily confirmed that the zone planes pass the points Γ and H in the first zone, when the sum of the Miller indices h, k, and l divided by 2 is even and odd, respectively.

The Fermi surfaces calculated from the E-k dispersions are shown in Fig. 6 in the reduced-zone scheme for the present approximant, together with the cross sections of free-electron Fermi spheres. The Brillouin zone in the k_xk_y plane is obviously bounded by the cross section of four (110) zone planes characteristic of its bcc structure. We can clearly see that many free-electron Fermi surfaces pass the point N but that the electronic states derived from the band calculations are strongly expelled from the area around the point N. This is certainly caused by the presence of finite energy gaps across the (543), (550), and (710) zone planes and can be taken as an additional evidence for the creation of the pseudogap at the Fermi level.

In conclusion, we have discussed the dispersion relations and the resulting Fermi surfaces derived from the LMTO-

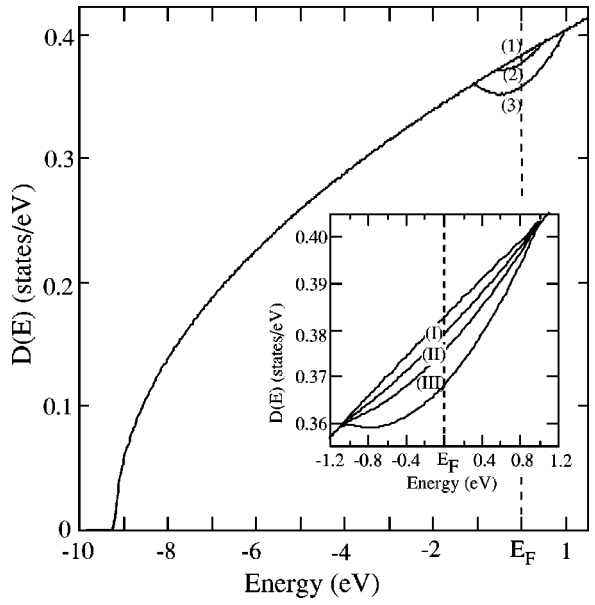

FIG. 5. Effect of deletion of the states enclosed by a sphere centered at the point N with radius Δk on the free-electron density of states. Curves (1), (2), and (3) refer to $\Delta k=0$, 0.1, and 0.2, respectively. Note that $\Delta k=0.2$, for example, ranges from 3.33 to 3.73 in Fig. 4. The DOS with $\Delta k=0.2$ is shown in its inset on expanded scale: (I), (II), and (III) show the contributions from the 12-folded (550), 24-folded (710), and 48-folded (543) zone planes, respectively.

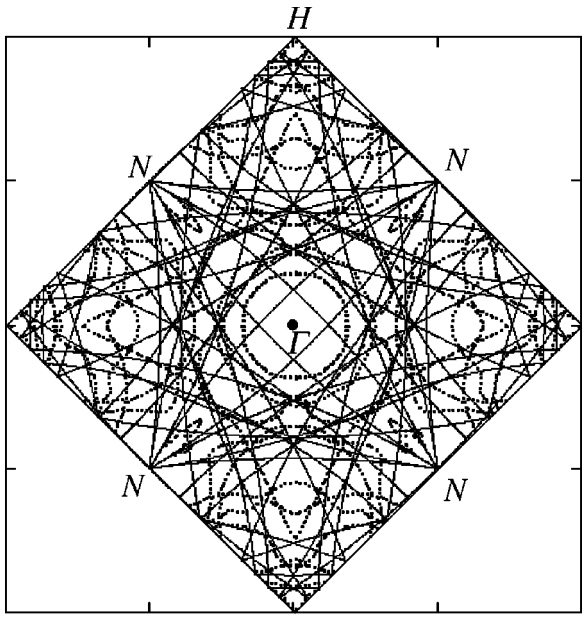

FIG. 6. Cross section of the Fermi surfaces calculated in the framework of the LMTO-ASA method and free-electron Fermi spheres cut across the k_xk_y plane in the reduced-zone scheme.

ASA band calculations with reference to those derived from the free-electron model in both extended- and reduced-zone schemes for the nearly-free-electron-like Al-Mg-Zn approximant and could prove that the pseudogap across the Fermi level originates from the interaction of the Fermi surfaces with the Brillouin zone formed by the (543), (550), and (710) zone planes associated with the observed strong x-ray diffraction peaks. We believe that the present work substantiated the empirical matching rule between the Fermi sphere and the Brillouin-zone planes from the first-principles band calculations and provided a firm basis for the Hume-Rothery rule. The extension of the present work to the MI-type QC's and AC's may not be straightforward because of the superposition of the *d* states near the Fermi level. The test of the validity of the Hume-Rothery matching rule based on the first-principles band calculations for the MI-type Al-Cu-Ru-Si AC is reported elsewhere.[17]

[1] A.P. Tsai, A. Inoue, Y. Yokoyama, and T. Masumoto, Mater. Trans., JIM **31**, 98 (1990).
[2] Y. Yokoyama, A.-P. Tsai, A. Inoue, T. Masumoto, and H.S. Chen, Mater. Trans., JIM **32**, 421 (1991).
[3] U. Mizutani, A. Kamiya, T. Matsuda, K. Kishi, and S. Takeuchi, J. Phys.: Condens. Matter **3**, 3711 (1991).
[4] T. Takeuchi and U. Mizutani, Phys. Rev. B **52**, 9300 (1995).
[5] T. Fujiwara, Phys. Rev. B **40**, 942 (1989).
[6] T. Fujiwara and T. Yokokawa, Phys. Rev. Lett. **66**, 333 (1991).
[7] J. Hafner and M. Krajčí, Phys. Rev. B **47**, 11 795 (1993).
[8] J. Friedel and F. Denoyer, C. R. Acad. Sci., Ser. II: Mec., Phys., Chim., Sci. Terre Univers **305**, 171 (1987).
[9] A.P. Smith and N.W. Ashcroft, Phys. Rev. Lett. **59**, 1365 (1987).
[10] V.G. Vaks, V.V. Kamyshenko, and G.D. Samolyuk, Phys. Lett. A **132**, 131 (1988).
[11] G. Trambly de Laissardiére, D. Nguyen Manh, L. Magaud, J.P. Julien, F. Cyrot-Lackmann, and D. Mayou, Phys. Rev. B **52**, 7920 (1995).
[12] V. Fournée, I. Mazin, D.A. Papaconstantopoulos, and E. Belin-Ferré, Philos. Mag. B **79**, 205 (1999).
[13] U. Mizutani, W. Iwakami, T. Takeuchi, M. Sakata, and M. Takata, Philos. Mag. Lett. **76**, 349 (1997).
[14] H. Nakano, Y. Sato, S. Matsuo, and T. Ishimasa, Mater Sci. Eng, A **294-296**, 542 (2000).
[15] O.P. Andersen, Phys. Rev. B **12**, 3060 (1975).
[16] H. L. Skriver, *The LMTO Method*, Springer Series in Solid-State Sciences Vol. 41, edited by M. Cardona, P. Fulde, and H.-J. Queisser (Springer, New York, 1984).
[17] U. Mizutani, T. Takeuchi, E. Banno, V. Fournée, M. Takata, and H. Sato, in *Quasicrystals*, edited by E. Belin-Ferré, P. A. Thiel, A.-P. Tsai, and K. Urban, Mater. Res. Soc. Symp. Proc. No. **643** (Materials Research Society, Pittsburgh, 2001).